

Microfacies, Biostratigraphy, Depositional Environment, Seismic Refraction and Correlation of Coralline Limestones of the Barzaman Formation (Oligocene-Pliocene? Al-Khod, Muscat Area, Sultanate of Oman)

Frank Mattern*, Abdul Razak Al-Sayigh, Mohammed Farfour, Andreas Scharf, Shaima Al-Amri and Juhaina Al-Omairi

Department of Earth Sciences, College of Science, P. O. Box 36, PC. 123, Al-Khod, Muscat, Sultanate of Oman, *Email: frank@squ.edu.om.

ABSTRACT: The "Carbonates" unit of the Oligocene-Pliocene Barzaman Formation, north of the Oman Mountains at Sultan Qaboos Campus, is at least 10 m thick. It consists of three coralline limestone beds in (1) bedded facies (base; eastern outcrop), (2) very thick-bedded debris facies (middle; western and eastern outcrops) and (3) bedded facies (top; western and eastern outcrops). These three beds can be correlated between two outcrops over a distance of 160 m based on facies, stratigraphic positions and thickness as well as on a seismic refraction survey. The most common bioclats are poritid corals, red algae and benthic foraminifers. Dasycladacean algae are common, and, sporadically, small gastropods, bryozoans, echinoderms, echinoid spines, bivalves, worm tubes and ostracods occur. Based on facies analysis we suggest that the studied limestones formed in a lagoon with backreef coral facies and that the barrier that separated the lagoon from the open sea (and which is not exposed) was made of coral reefs. Because of the abundance of coral colonies we assume for the studied coral limestones a water depth within the light saturation zone, not deeper than 10 to 20 m for the lagoon. Based on the occurrence of the following foraminifer genera *Praerhapydionina*, *Archaias*, *Dendritina*, *Operculina*, *Spiroclypeus*, *Lepidocyclina*, *Miogypsina*, *Amphistegina* and *Subterraniophyllum*, the "Carbonates" unit can be dated as upper Upper Oligocene to Lower Miocene. This is the first indication of the Upper Oligocene of the Barzaman Formation for the study area.

Keywords: Benthic foraminifers; Poritid corals; Red algae; Debrite; Debris flow; Lagoon.

السحنات الدقيقة، الطبقة الحياتية، البيئات الرسوبية، الانكسارات السيزمية والمضاهاة للحجر الجيري المرجاني لتكوين برزمان (الأوليغوسين الباليوسين الخوض منطقة مسقط عمان)

فرانك مارتن، عبدالرزاق الصايغ، محمد فرفور، أندرياس، شيماء العامري، جهينه العريمي

الملخص: يبلغ سمك وحدة "الكربونات" في تكوين برزمان، شمال جبال عمان، 10 أمتار على الأقل. وهو يتكون من ثلاثة طبقات من الحجر الجيري المرجاني سحنة متطبقة في الأسفل سحنة حطام سميكة للغاية في الوسط وسحنة متطبقة في الأعلى. هذه الثلاث طبقات يمكن مضاهاتها بين مكشوفين على مسافة تصل إلى 160 مترًا على أساس 14 خصائص صخرية/سحنية، مواقع التتابع الطبقي والسمك، كما الحال في 15 أنظمة انكسارات السيزمية اعتبارات الخصائص الصخرية/السحنية، مواقع الطبقة المناظرة والسمك. الشظايا الصخرية الحياتية الأكثر شيوعًا هي المرجان المسامي، والطحالب الحمراء والمنخربات القاعية. الطحالب الداسيكلاديشانية شائعة، وتحدث بشكل متقطع بطبقات المعدة الصغيرة، البريزوزانات، القنفذيات، محور فقاعي، ذوات الصدفتين، الانابيب الدودية، و الأوستراكوذا. استنادًا إلى اعتبارات السحنات الحياتية على سبيل المثال، وجود المعيار السحني الحياتي، فإننا نقترح أن الحجر الجيري الذي تشكل في البحيرة وأن الحاجز الذي يفصل بحيرة عن البحر المفتوح يتكون من الشعاب المرجانية. بسبب وفرة المستعمرات المرجانية، فإننا نفترض عمقًا مائيًا داخل منطقة تشبع الضوء، لا يتجاوز عمقها من 10 إلى 21 مترًا للبحيرة. استنادًا إلى تواجد الأشكال التالية من منخربات اركايس، دندريتين، ابركولينا، سبيروكليبيوس، لبيدوسيكلينا، ميوجيبسينا، أمفستيجينا سبترانيفيلم، تؤرخ وحدة "الكربونات" للعمر الأوليغوس العلوي لغاية الميوسين (الميوسين السفلي-العلوي). هذا يعتبر أول دليل أن تكوين برزمان يرجع للعمر الأوليغوسيني المتأخر لمنطقة الدراسة على نطاق واسع.

الكلمات المفتاحية: المنخربات القاعية، الشعاب المرجانية المسامية، الطحالب الحمراء، السبيكة، تدفق الحطام، البحيرة.



1. Introduction

The Barzaman Formation was defined south of the Oman Mountains [1, 2]. The formation in its type locality is made of several hundred meters thick carbonates and conglomerates and formed within alluvial fans of assumed Pliocene-Pleistocene age [1, 2]. Parts of the Barzaman Formation west of the Northern Oman Mountains, in the UAE, may have formed by debris flows during pluvial episodes [3]. The Barzaman Formation was also deposited during an enhanced exhumation phase of the Oman Mountains during the Late Miocene [4]. Most of the formation is exposed south or west of the Oman Mountains, which makes the outcrops in our study area rare and special.

For a long time, the Barzaman Formation of the study area near Al-Khod (Muscat/Seeb area) has not attracted any detailed research activities. Accordingly, the Geological Map of Seeb and the respective Explanatory Notes [5] lack a comprehensive description of the formation. The provided age information is vague (“Middle’ Miocene to probably Pliocene”), the thickness is quantified to be 100 m, and the lithology is summarized as consisting of white to reddish conglomerate, sandstone, shale and chalky limestone [5]. However, recently, a single sedimentary log of the Barzaman Formation with coralline limestones from the campus of Sultan Qaboos University (SQU) was published [6], and a lithostratigraphic correlation of the formation was established for the campus based on a number of stratigraphic logs located at different places [7]. The limestones form the second out of five lithostratigraphic units of the Barzaman Formation cumulatively referred to as “Carbonates”, and contain a variety of benthic foraminifers. The limestones are exposed in the western part of SQU campus.

On the campus, the limestone unit is exposed at a car park, immediately to the west of the College of Economics and Political Science in two places: to the west and to the east of the car park (Fig. 1A and B). While [6] interpreted the two limestone occurrences as being of different ages and depicted them in vertical succession, [7] correlated them laterally. There are reasons for these inconsistent interpretations: the geological structure is unclear. While along the southern margin of the car park (outcrop not marked in Figure 1) the layers of the Barzaman Formation are exposed in a cross section (dip orientation), the beds of the formation along the northern margin of the car park (outcrop not marked in Fig. 1) are exposed along a strike section although both outcrop sections are parallel. Moreover, there is a syndepositional thrust at the northern outcrop [7]. In addition, the road surface of the parking area covers the critical transitional area between the two outcrops and renders its visual analysis impossible. What further complicates the stratigraphic understanding is the incomplete stratigraphic record in both limestone sections at an erosional truncation surface and an onlap relationship, respectively.

This study was carried out to resolve the inconsistent interpretations of the stratigraphic relationship between the two limestone outcrops by studying their facies/microfacies and used a seismic refraction survey to possibly elucidate the geological structure beneath the car park as an additional tool to solve the problem. Since the limestones contain different benthic foraminifers [7] we extend the microfacies investigation of the fossiliferous limestones to date the foraminifers as the age of the Barzaman Formation was previously poorly understood.

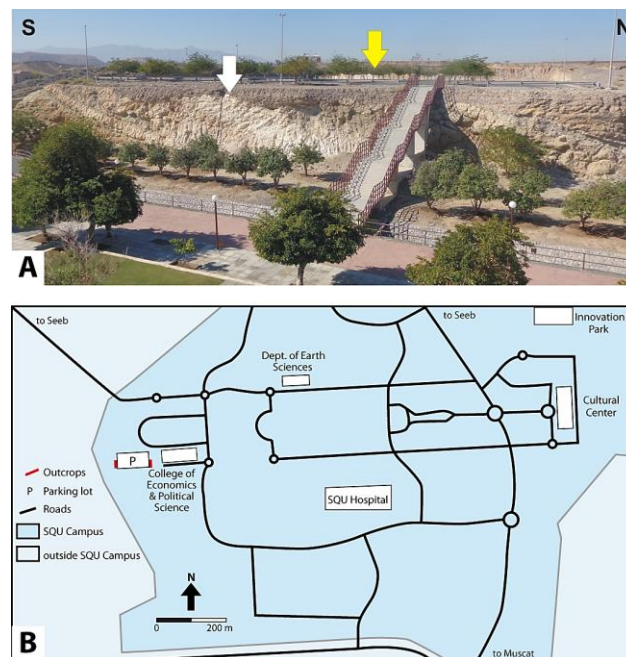


Figure 1. Locations of the two studied outcrops. **A.** View to the west across the car park west of the College of Economics and Political Science with the outcrops of the Barzaman Formation on the SQU campus with exposed coralline limestones. The car park occupies a plateau-like area. The outcrop in the west (background, yellow arrow) is located at the car park level while the outcrop in the east (foreground, white arrow) is below the car park. Scale is

GEOLOGY OF THE BARZAMAN FORMATION

indicated by stairway with 60 stairs. For the size of the parking lot see Figure 1B. **B.** Road system of SQU campus and locations of the two coralline limestone outcrops of the Barzaman Formation.

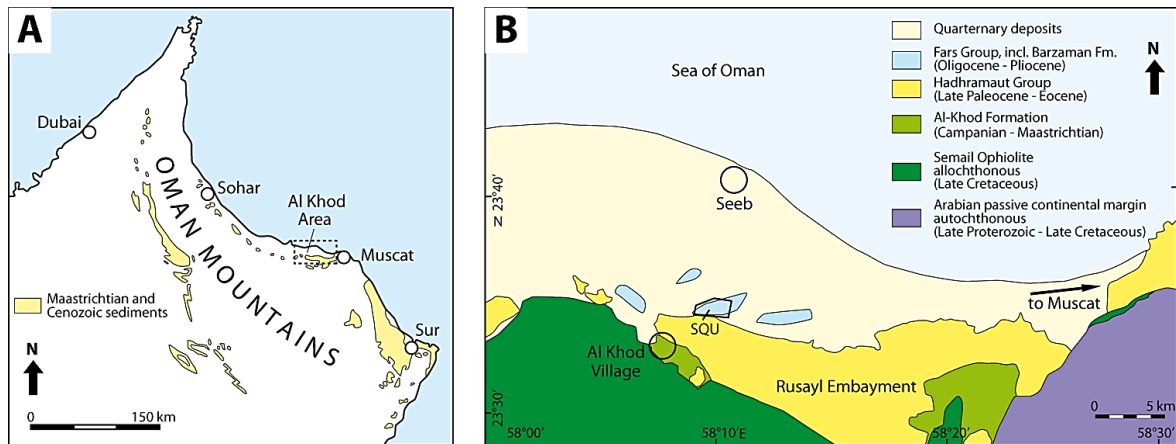


Figure 2. Geological setting of the study area. **A.** Outcrops of Maastrichtian and Cenozoic post-obductional sediments of northern Oman. Note how these sediments surround the Oman Mountains! Modified after [8, 5]. Box with dotted lines shows the location of the map of B. **B.** Simplified geological map of the greater study area. The study area is shown in the dotted box of A. SQU-Sultan Qaboos University campus. Modified from [9].

2. Geological Setting

The Cenozoic geological setting of the Barzaman Formation postdates formation of the Oman Mountains which resulted from the Late Cretaceous obduction of the Tethys-derived Semail Ophiolite as well as Tethyan ocean floor sediments (Hawasina Group) during closure of the Tethys Ocean, which also caused formation of large dome structures in the newly created mountain belt [10-18]. Two of these nearby domes are the Jabal Akhdar and Saih Hatat domes. Eocene to Miocene exhumation has been reported for both domes [19]. Both domes are flanked by a major extensional fault zone which was active during exhumation of the two domes [20]. The Barzaman Formation may have accumulated during exhumation of the two domes.

Following the interval of mountain building, Cenozoic deposition ensued marginally to the mountains (Figure 2A), including the Rusayl Embayment to which the study sites belong (Figure 2B). Most Cenozoic sediments are marine and measure several hundred meters in cumulative thickness [8, 5]. Late Paleocene to Oligocene sediments accumulated in overall stable, shallow marine conditions [21] as slow subsidence affected the area from the Eocene to the Oligocene [22]. During deposition of the Barzaman Formation, syndepositional thrusting is documented [7]. The Barzaman Formation is subdivided into the following lithostratigraphic or facies units [7]:

5. Dolomitic Conglomerates (top) / > 60 m thick
4. Claystones and Conglomerates / 19 m thick
3. Varied Thick Sandstones and Conglomerates / 10-35 m thick
2. Carbonates / >10m thick and
1. Lower Conglomerates and Sandstones / >35 m thick (base).

3. Methods

We collected 14 limestone samples from both outcrops and analyzed them in thin sections with transmitted light microscopy regarding their microfacies and foraminifer content. Moreover, a seismic refraction survey was carried out to map and delineate the near-surface interval of the formation. The seismic survey was designed in such a way that the uppermost 20 meters of the near-surface structure could be reached and imaged. The survey consists of 4 profiles (see section 4.4) which are 20 m apart, each with 5 shots. The spacing between geophones was 3 m and all lines are 70 m long. We used a hammer as the energy source. The profiles were run from west to east. After data collection, the first arrival times for the shots were picked and used for inversion. After several inversion iterations, a velocity model was obtained for each line.

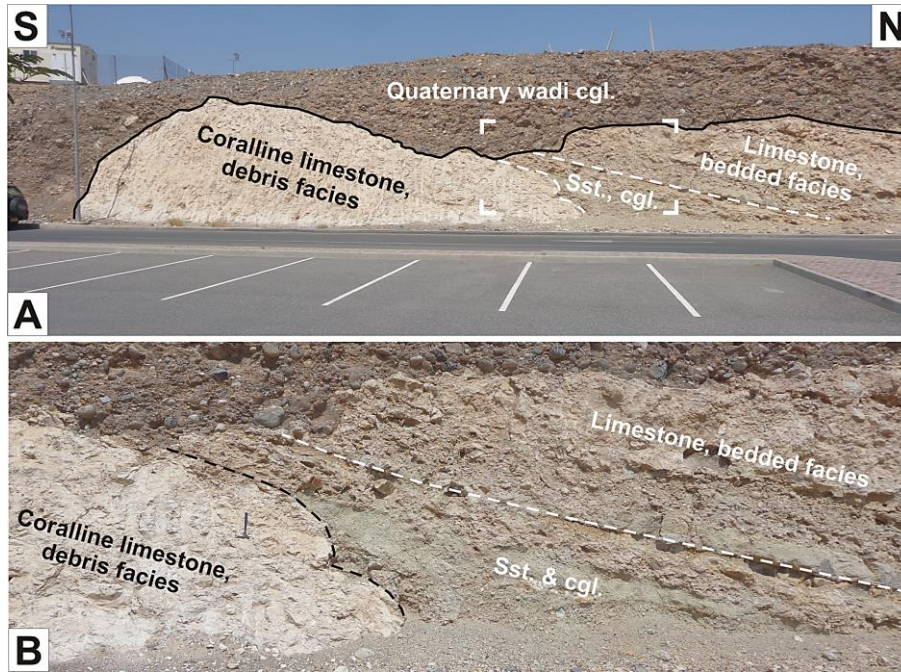


Figure 3. Western outcrop. Sst-sandstone; Cgl-conglomerate. **A.** Overview with the tilted beds of the Barzaman Formation overlain at an angular unconformity (black line) by Quaternary wadi conglomerate. The white box outlines the detail shown in B. Back of car (left) for scale. **B.** Detail of the outcrop marked by box in A. The close-up emphasizes the onlap of sandstone and conglomerate beds against the steeper surface of the coralline limestone (debris facies) to the south. Note how the sandstone and conglomerate beds terminate at the coralline limestone! Hammer (35cm long) for scale.

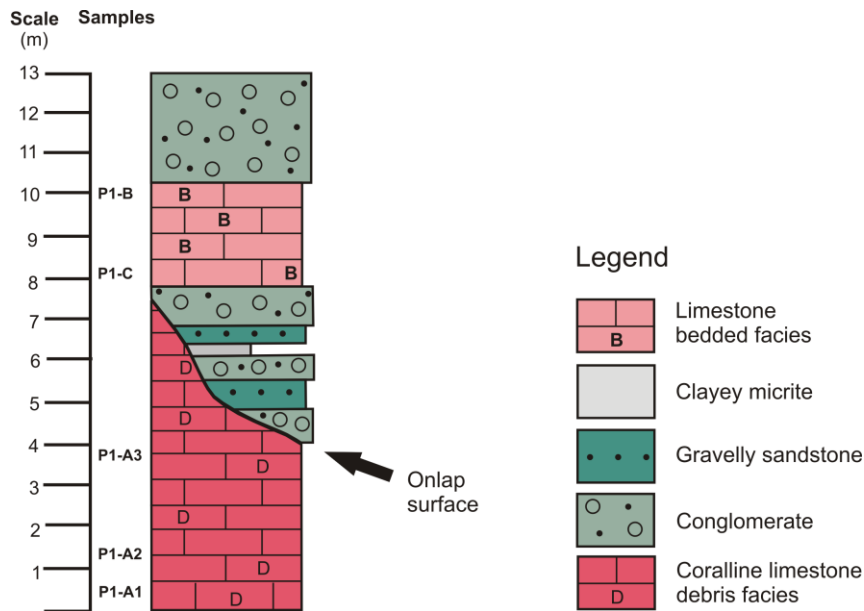


Figure 4. Stratigraphic log of the western outcrop with sample locations.

4. Results

4.1 Western Outcrop

4.1.1 Field Results and Sedimentary Log

The western outcrop (coordinates: 23°35'21.03"N / 58° 09'35.32"E) exposes limestone, conglomerate and sandstone of the Barzaman Formation. The Barzaman Formation is tilted and overlain by Quaternary wadi conglomerate along an angular unconformity (Figures 3A and B).

GEOLOGY OF THE BARZAMAN FORMATION

The oldest exposed bed of the Barzaman Formation in this outcrop is the white to beige coralline limestone (Fig. 3A). The maximum thickness of this very thick-bedded layer is uncertain as its base is not exposed (Figure 3A). The minimum bed thickness is 7.5 m. The limestone is characterized by indistinctly massive bedding and the occurrence of numerous cobbles and boulders of coral colonies which display an orientation in normal growth position, or they are toppled or are upside down. Some of the coral fragments exhibit selective silicification by brown, hematitic silica which makes the silicified colonies easy to identify in the field.

The massive character and the coral fragments of different orientations identify this limestone unit as a coral-dominated debris deposit/carbonate breccia. This result is further supported by the fact that the debris deposit has a lateral slope against which the sandstone and conglomerate beds onlap (Figs. 3B and 4).

There are three thick-bedded conglomerate layers with matrix-supported clasts. The conglomerate is polymictic, and the clasts are subrounded, poorly sorted and mainly of granule to pebble size (Figures 3B and 4). The clast types are cherts and igneous rocks of the Hawasina Group and Semail Ophiolite origin, respectively. The conglomerates are marine as indicated by the occurrence of a solitary coral. The conglomerates are associated with two thick gravelly sandstone beds (Figures 3B and 4) with 25% of gravel clasts and also a thin bed of clayey micrite (Figure 4).

The clastic deposits are overlain by bedded coralline packstone (at places also boundstone to rudstone) cumulatively measuring 2.5 m in thickness. These beds contain fragments of coral colonies. The bedded limestone is then overlain by sandstone and conglomerate of the Barzaman Formation (Figures 3 and 4).

4.1.2 Microscopic Results (Microfacies)

All thin sections are characterized by a micrite matrix. They contain the following bioclasts listed in terms of their overall frequency (estimates): 1. Very common: poritid corals, benthic foraminifers, red algae. 2. Common: small gastropods, echinoid spines, dasycladacean algae. 3. Sporadic: bryozoans, bivalves, worm tubes.

Among the red algae are both encrusting and non-encrusting types. Red algae may encrust dasycladacean algae. Worm tubes may encrust corals (Figure 5B).

According to the microfacies analyses, we can interpret the massive coralline boundstone at the base of the formation as redeposited material on a slope whereas the bedded corallite-bioclastic limestone beds correspond to Standard Microfacies 18 (SMF18) and to Facies Zone 7 (FZ7) of [23] (see P1-B and P1-C in Table 1), suggesting lagoonal conditions.

Table 1. Summary of thin section analyses of samples from the western outcrop in stratigraphic order (base at bottom). The Standard Microfacies (SMF) and Facies Zones (FZ) correspond to the system of [23]. Limestone and SMF classifications must be understood with caution if sample is from a debris.

Sample; facies	Bioclasts in approximate order of frequency; other components	Limestone classification	SMF/FZ
P1-B; Bedded	Poritid corals, benthic foraminifers, dasycladacean algae, red algae, bryozoans	Packstone	18/7
P1-C; Bedded	Poritid corals, benthic foraminifers, dasycladacean algae, red algae, echinoid spines	Packstone	18/7
P1-A3; Debris	Poritid corals, benthic foraminifers, red algae, worm tubes; Igneous lithoclasts (ophiolite) and detrital quartz	Packstone to boundstone	-/-
PA-A2; Debris	Poritid corals, dasycladacean algae, bivalves, red algae, small gastropods, worm tubes	Packstone	-/-
PA-A1; Debris	Benthic foraminifers, red algae, small gastropods, poritid corals, echinoid spines, dasycladacean algae	Packstone	18/7

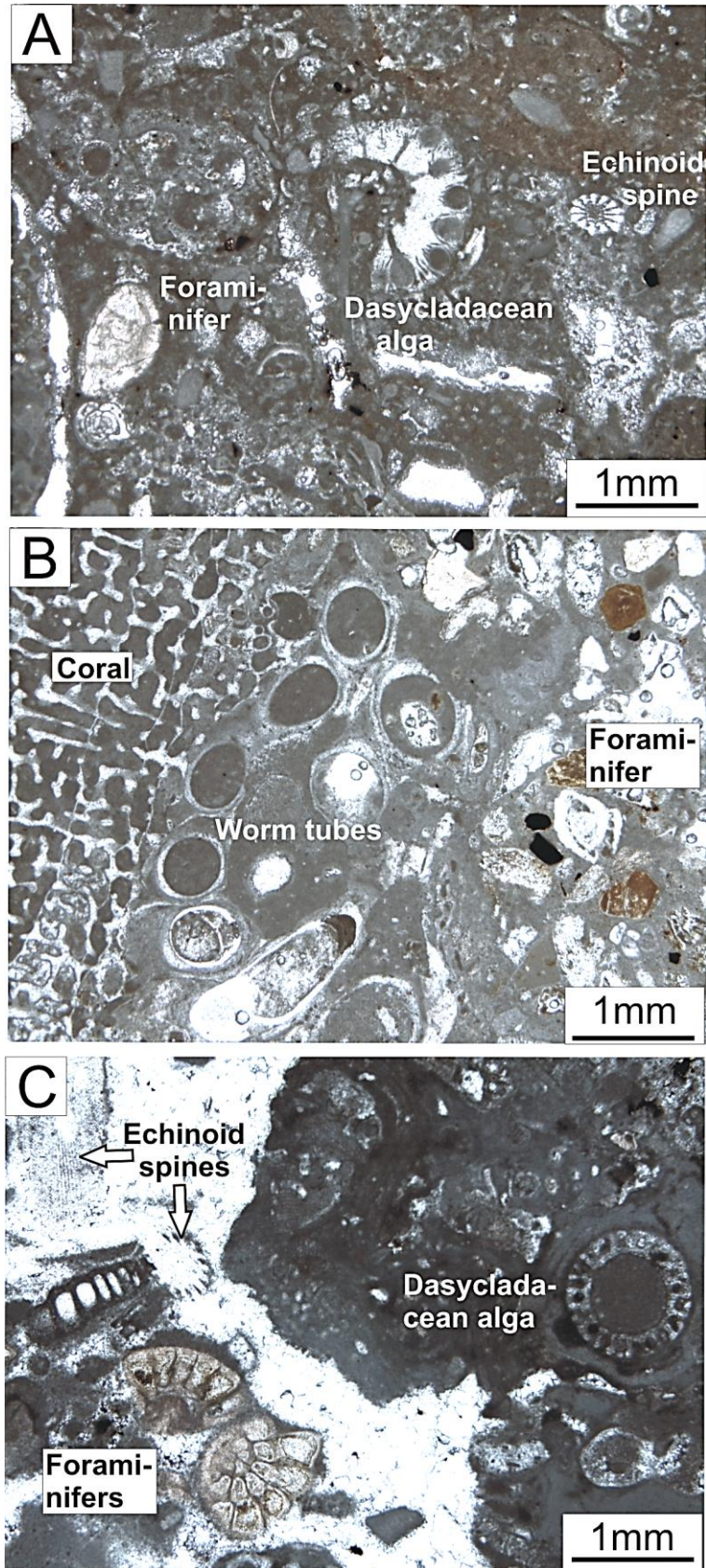


Figure 5. Thin sections (all PPL) from the limestones of the western outcrop with typical bioclast associations. **A.** Debris facies with benthic foraminifer, dasycladacean alga and echinoid spine (sample P1-A1). **B.** Debris facies with poritid coral, worm tubes which are encrusting the coral and benthic foraminifer (sample P1-A3). **C.** Bedded facies with benthic foraminifers, dasycladacean alga and echinoderm spines. This sample corresponds to SMF18 and FZ7 (sample P1-A3).

GEOLOGY OF THE BARZAMAN FORMATION

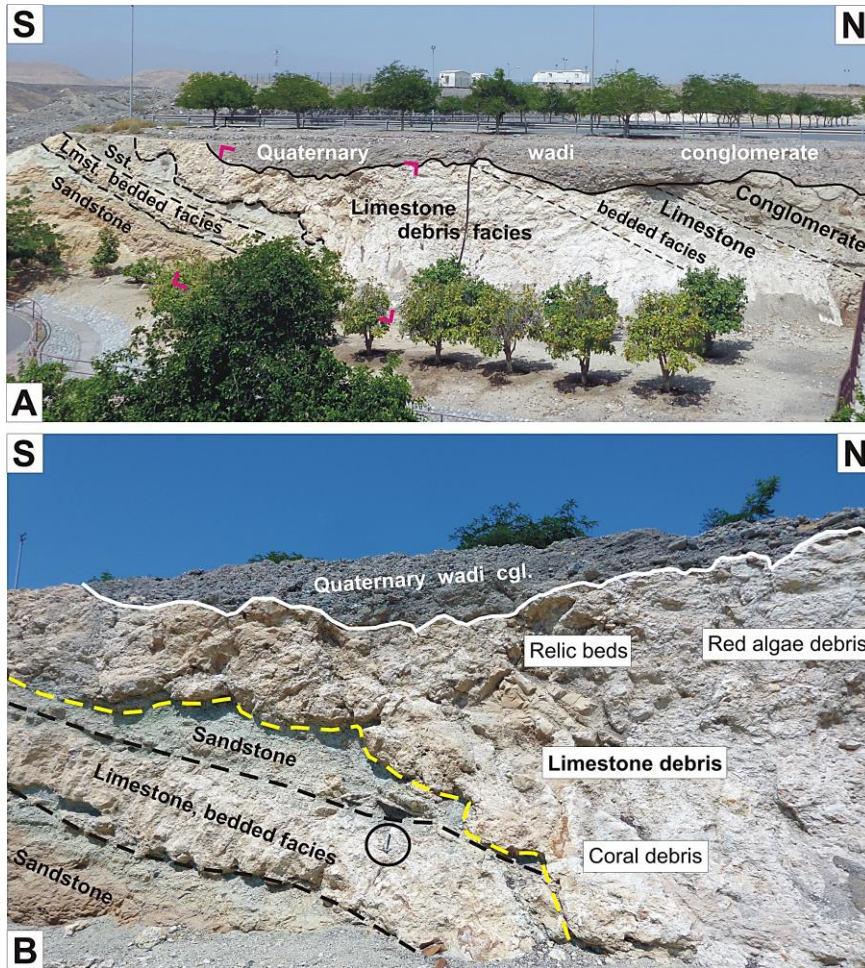


Figure 6. Eastern outcrop. **A.** Overview of the tilted beds of the Barzaman Formation below an angular unconformity (black line) by Quaternary wadi conglomerate. The red box outlines the detail shown in B. The stairway on the right is the same as the in Figure 1A. **B.** The detail of the outcrop is marked by the red box in A. The detail emphasizes downcutting of the limestone debrite into sandstone and conglomerate as well as into the bedded limestone (yellow dashed line). The different kinds of debris form irregularly shaped domains. The short relic beds consist of clayey micrite. The angular unconformity is marked by the white line. Note how the sandstone and limestone beds terminate at the limestone debrite. Hammer (length 35 cm) for scale.

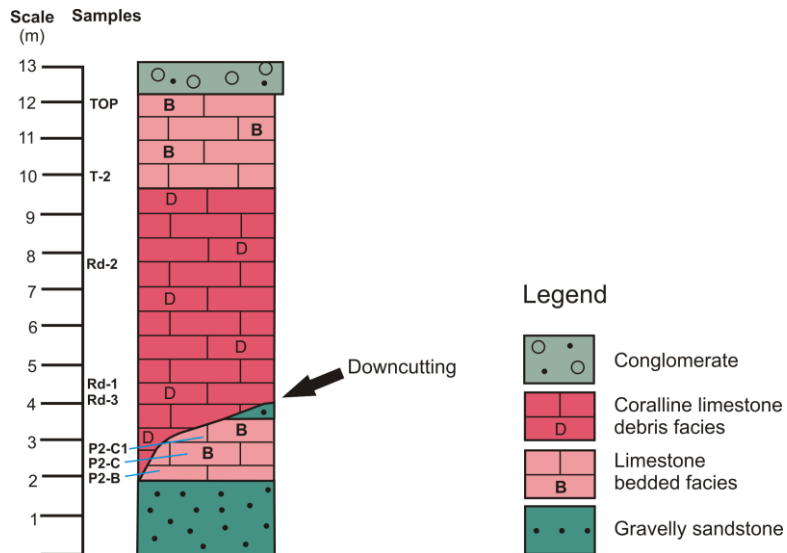


Figure 7. Stratigraphic log of the eastern outcrop with sample locations.

4.2 Eastern Outcrop

4.2.1 Field Results and Sedimentary Log

The eastern outcrop (coordinates: 23°35'22.38"N / 58° 09'40.88"E) also exposes limestone, conglomerate and gravelly sandstone of the Barzaman Formation. The layers are tilted and overlain by Quaternary wadi conglomerate at an angular unconformity (Figures 6A and B).

This outcrop shows beds belonging to the oldest of the five lithostratigraphic units of the Barzaman Formation, namely the siliciclastic rocks of the “Lower Conglomerates and Sandstones” of [7]. They are represented in Figs. 6 and 7 by the depicted brown (base and center) and greenish (top) basal gravelly sandstone similar in composition and texture to the ones of the western outcrop.

Above the basal sandstone the oldest limestone bed of the Barzaman Formation follows. It is a light-colored, bedded, coralline boundstone (at places grainstone). It contains selectively silicified brown, hematitic, dm-scale coral colonies. It is overlain by a greenish gravelly sandstone bed. Both the limestone and sandstone are laterally cut off by the erosive base of the overlying very thick-bedded limestone debris (Figure 6B).

The very thick-bedded limestone layer is beige to white and characterized by chaotic bedding. It features toppled cobbles of coral colonies. The chaotic bedding is also perceivable by irregularly shaped zones of predominantly coral debris and red algae debris as well as the presence of short relic beds of clayey micrite (Figure 6B). Some of the coral fragments exhibit selective silicification by brown, hematitic silica, which makes these coral colonies easy to identify. Taking into account the chaotic nature of the very thick-bedded limestone and the fact that it cuts down into the subjacent layers, this bed may be interpreted as a gravity mass flow deposit with an erosive base. Since the base of the bed is not exposed, the total unit cannot be determined. The minimum thickness is 7.5 m.

This deposit is overlain by a white to gray bedded coralline boundstone (Figures 6A and 7) which contains numerous coral fragments that can be identified in the field. It is overlain by a conglomerate of the next lithostratigraphic unit of [7], the “Varied Thick Sandstones and Conglomerates”. This conglomerate is similar to the ones of the western outcrop.

4.2.2 Microscopic Results (Microfacies)

The lower bedded coralline limestone is partly micritic and partly sparitic. The chaotic debris limestone is micritic except for sample Rd-3. The upper bedded limestone is a micrite. The limestones contain the following bioclasts listed in terms of their overall frequency: 1. Very common: poritid corals, red algae, benthic foraminifers. 2. Common: dasycladacean algae. 3. Sporadic: echinoderm debris, bivalves, echinoid spines, small gastropods, ostracods. Among the red algae are encrusting and non-encrusting types.

Table 2. Summary of thin section analyses of samples from the eastern outcrop in stratigraphic order (base at bottom). The Standard Microfacies (SMF) and Facies Zones (FZ) correspond to the system of [23]. Limestone and SMF classifications must be understood with caution if sample is from a debris.

Sample; facies	Bioclasts in approximate order of frequency, other components	Limestone classification	SMF/FZ
TOP; Bedded	Red algae, benthic foraminifers, echinoderms, ostracods	Wackestone	-/-
T-2; Bedded	Poritid corals, red algae, dasycladacean algae, benthic foraminifers,	Boundstone	-/-
Rd/2; Debris	Poritid corals, red algae	Boundstone	-/-
Rd/1; Debris	No bioclasts; Highly altered lithoclasts (igneous ophiolite) and one fine pebble size radiolarite fragment	Wackestone	-/-
Rd/3; Debris	Red algae, benthic foraminifers, poritid corals, small gastropods, dasycladacean algae; bivalves, echinoid spines; Different limestone lithoclasts	Grainstone	18/7
P2-C1; Bedded	Poritid corals (whole sample)	Boundstone	-/-
P2-C; Bedded	Poritid corals, different benthic foraminifers, red algae; Peloids, micritic lithoclasts	Grainstone	-/-
P2-B; Bedded	Poritid corals (whole sample)	Boundstone	-/-

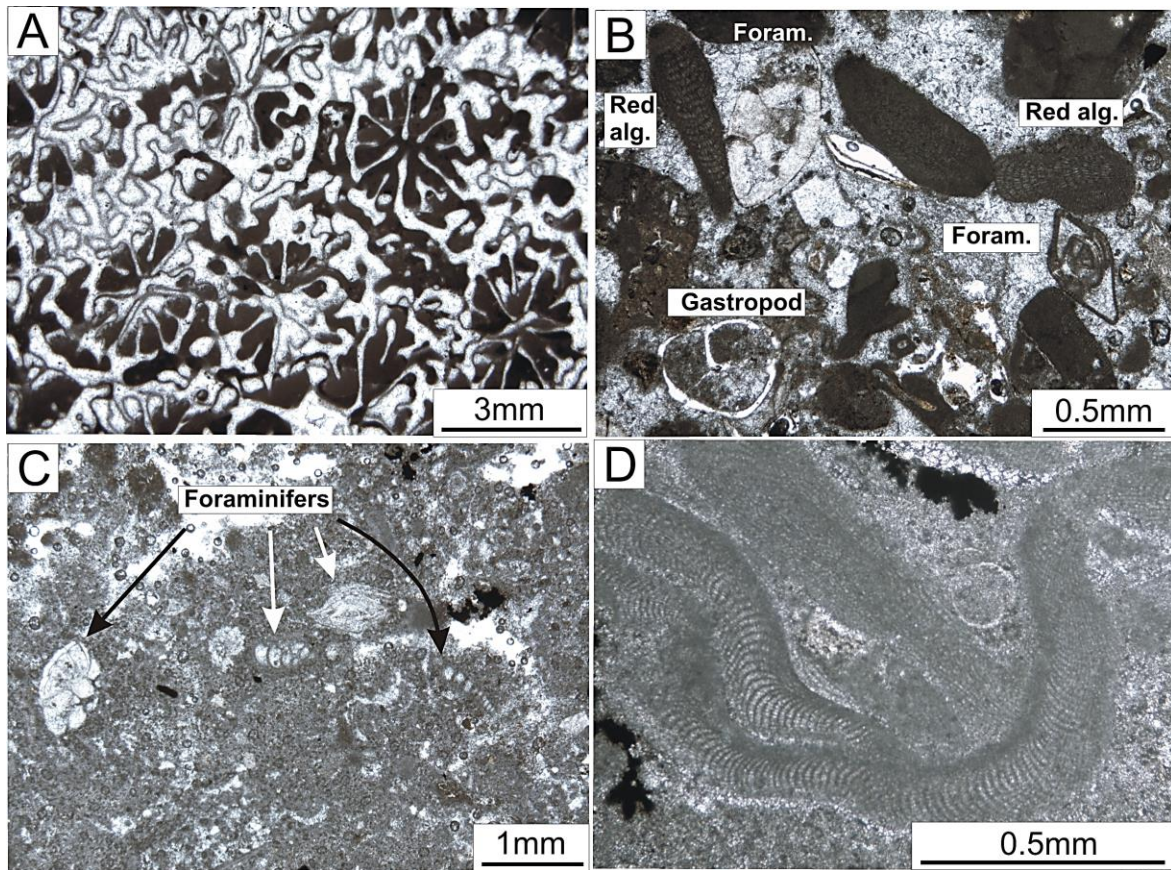


Figure 8. Thin sections (all PPL) from the limestones of the western outcrop with typical bioclasts. **A.** Bedded facies from the lower bedded limestone with poritid corals mainly in transverse section (sample P2-B). **B.** Debris facies with benthic foraminifers, red algae and a small gastropod (sample Rd-2). **C.** Bedded facies from the upper bedded limestone with benthic foraminifers (sample TOP). **D.** Bedded facies from the upper bedded limestone with red algae (sample TOP).

4.3 Biostratigraphic Results (Eastern and Western Outcrop)

The studied limestones contain a variety of benthic foraminifers among which *Amphistegina* and *Operculina* are the most common genera. The identified forms of benthic foraminifers are *Praerhapydionina*, *Archaias*, *Dendritina*, *Operculina*, *Spiroclypeus*, *Lepidocyclina*, *Miogypsina*, *Amphistegina* and *Subterraniophyllum*. They are listed in Figure 9 with their biostratigraphic occurrence, according to [24]. According to their age range, these genera and species indicate that the limestones of the Barzaman Formation represent the Oligocene and Miocene (Figure 9). Since *Miogypsina* represents the Upper Oligocene and Lower Miocene and temporally overlaps with all other genera, the studied limestone section is of Upper Oligocene to Lower Miocene age. The overlap between *Subterraniophyllum* and *Miogypsina* seems to indicate the presence of the Upper Oligocene.

4.4 Seismic Refraction Survey

Of the four profiles (P1 to P4; Figure 10) we will refer to only three (P2 to P4) as this is sufficient to summarize and justify our results. The observation of inverted sections inferred that velocities vary with depth. These velocities typically express the speed of seismic waves in the rocks which is directly related to the elastic properties of each rock type. The velocities vary also laterally along the same profile which indicates variation in the morphology of the layers and their petrophysical properties (e.g., porosity).

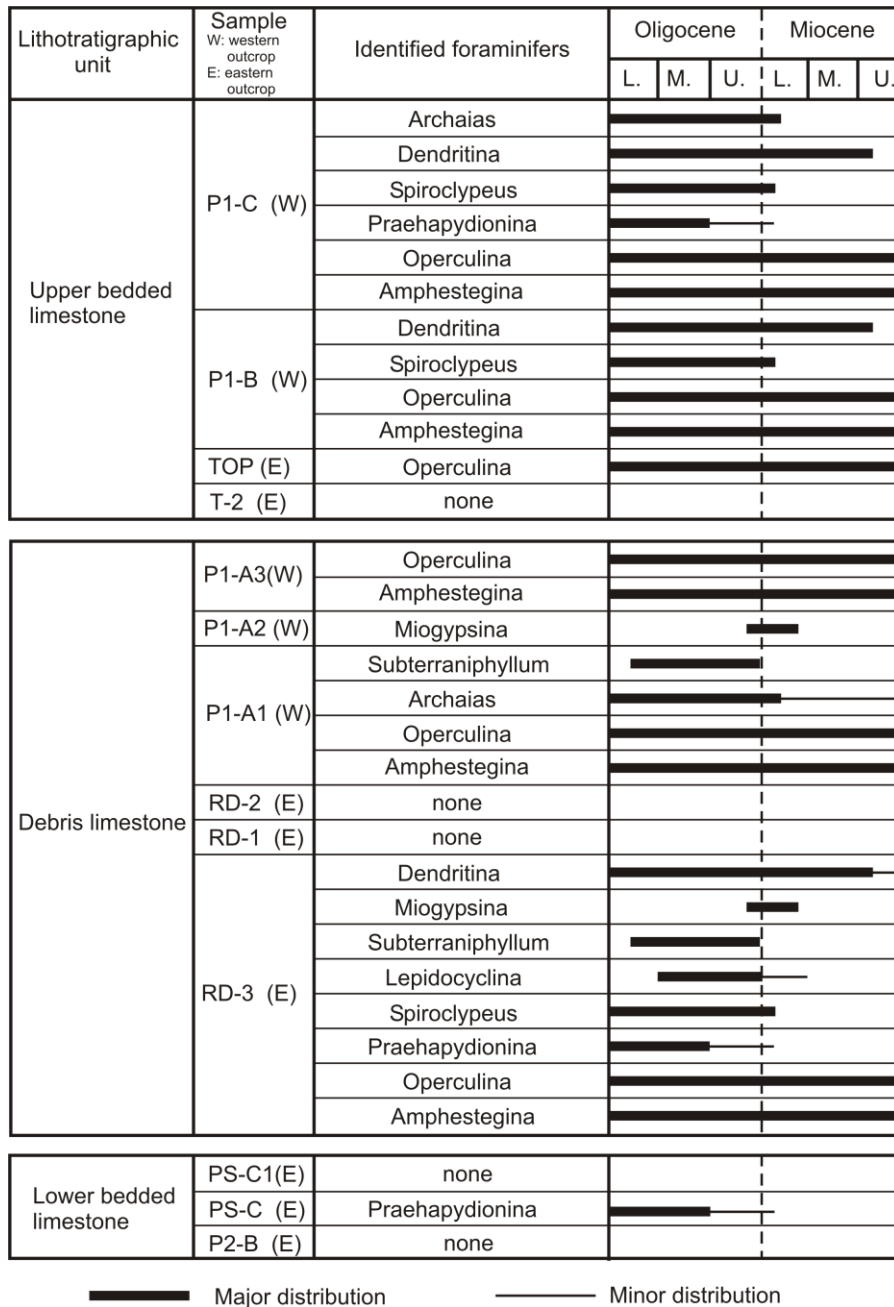


Figure 9. Identified benthic foraminifers in the thin sections and their stratigraphic ranges, according to [24]. The samples from the western outcrop are marked with “(W)” and those from the eastern outcrop with “(E)”. All eastern and western samples are listed from old (bottom) to young (top). There are nine genera of benthic foraminifers in the studied limestone beds. Note that *Miogypsina*, representing the Upper Oligocene and Lower Miocene, temporally overlaps with all other genera! Also note the narrow overlap between *Subterraniophyllum* and *Miogypsina*.

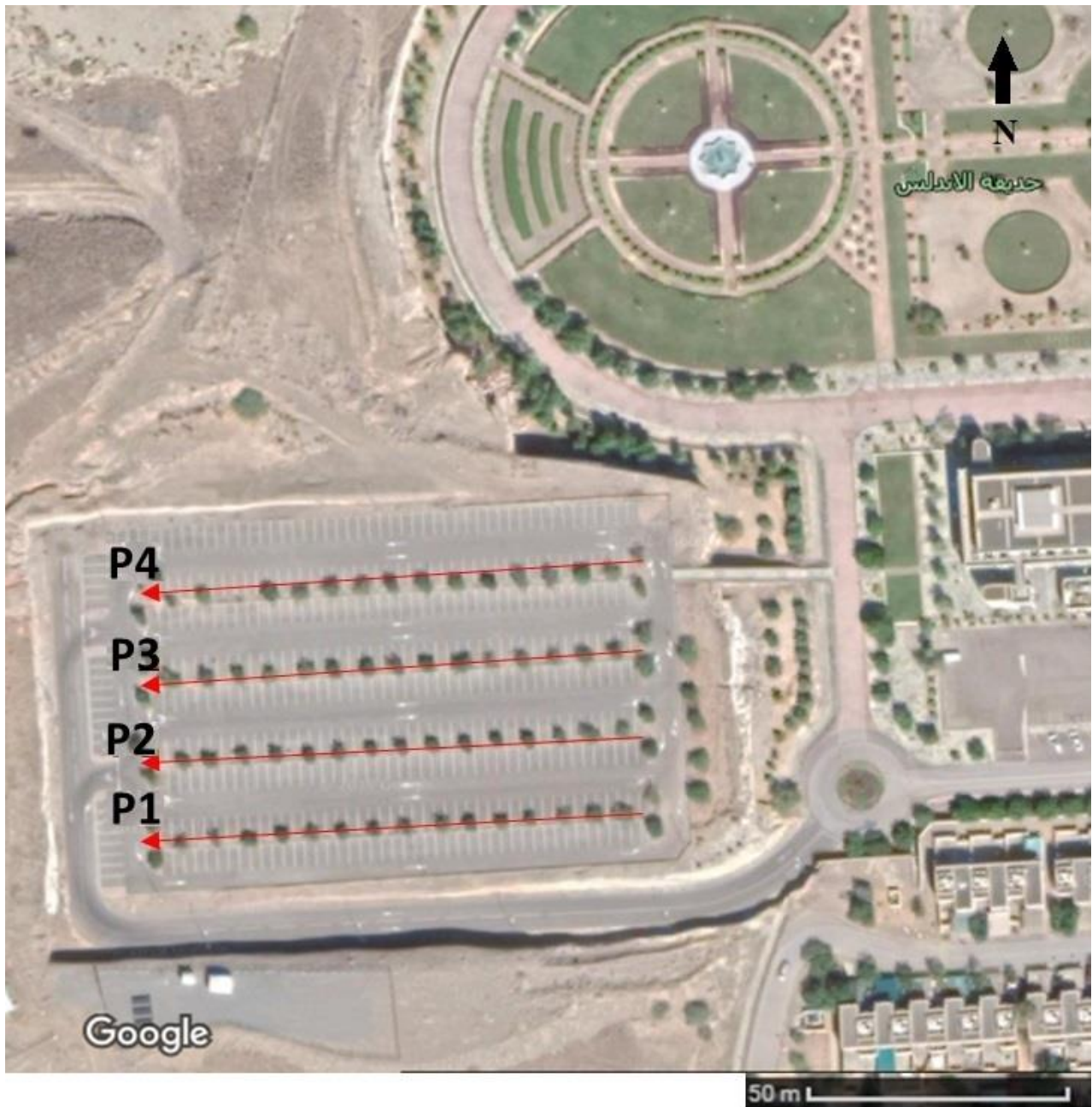


Figure 10. Satellite image showing the seismic refraction profiles P1 to P4 on the parking lot. For location of the parking lot see “P” in Figure 1B.

It was noticed that the “Carbonates” are dipping to the north so that they become absent in Profile 04 (Figures 11 to 13). The layers also dip gently to the east (Figures 11 to 13). In addition, the survey revealed some gentle wave-like folding of the Barzaman Formation (Figures 11 to 13). The layer structure as shown in the Figures 11 to 13 further demonstrates that the “Carbonates” form continuous horizons from west to east. The “Carbonates” in the western outcrop also appear in the eastern outcrop. The thickness of the “Carbonates” increases slightly to the east.

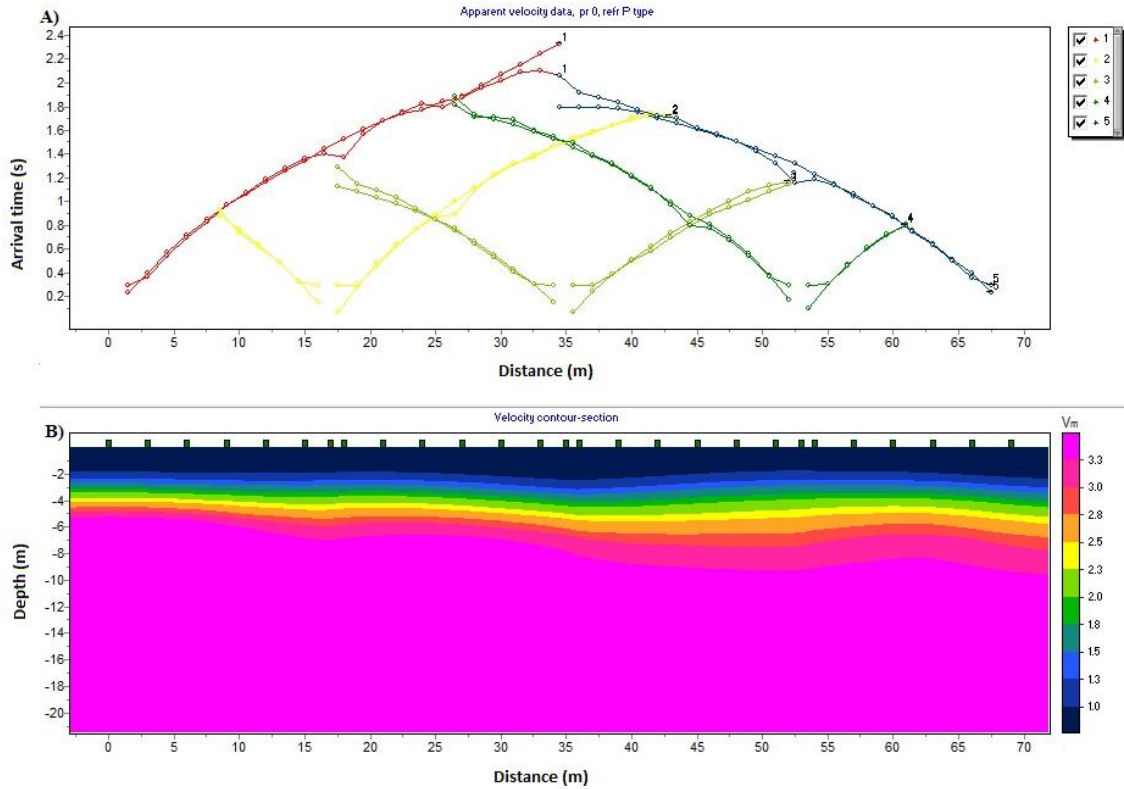


Figure 11. Seismic Refraction Profile P2.

A. Arrival times of the seismic waves as received by the geophones, plotted in time and distance.

B. Velocity model. The yellow and orange horizons represent the “Carbonates”. The blue and green horizons on the one hand and the red horizon on the other hand represent the overlying and subjacent clastic rocks, respectively.

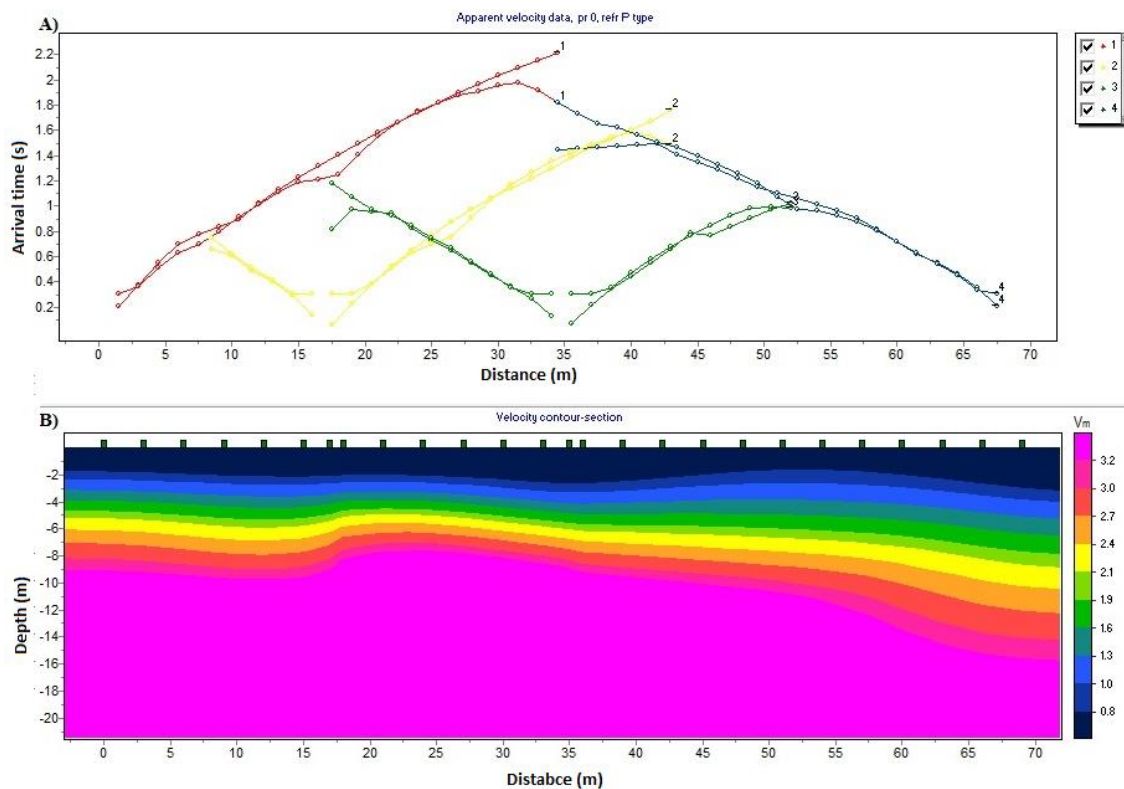


Figure 12. Seismic Refraction Profile P3.

A. Arrival times of the seismic waves as received by the geophones, plotted in time and distance.

B. Velocity model. The yellow and orange horizons represent the “Carbonates”. The blue and green horizons on the one hand and the red horizon on the other hand represent the overlying and subjacent clastic rocks, respectively.

GEOLOGY OF THE BARZAMAN FORMATION

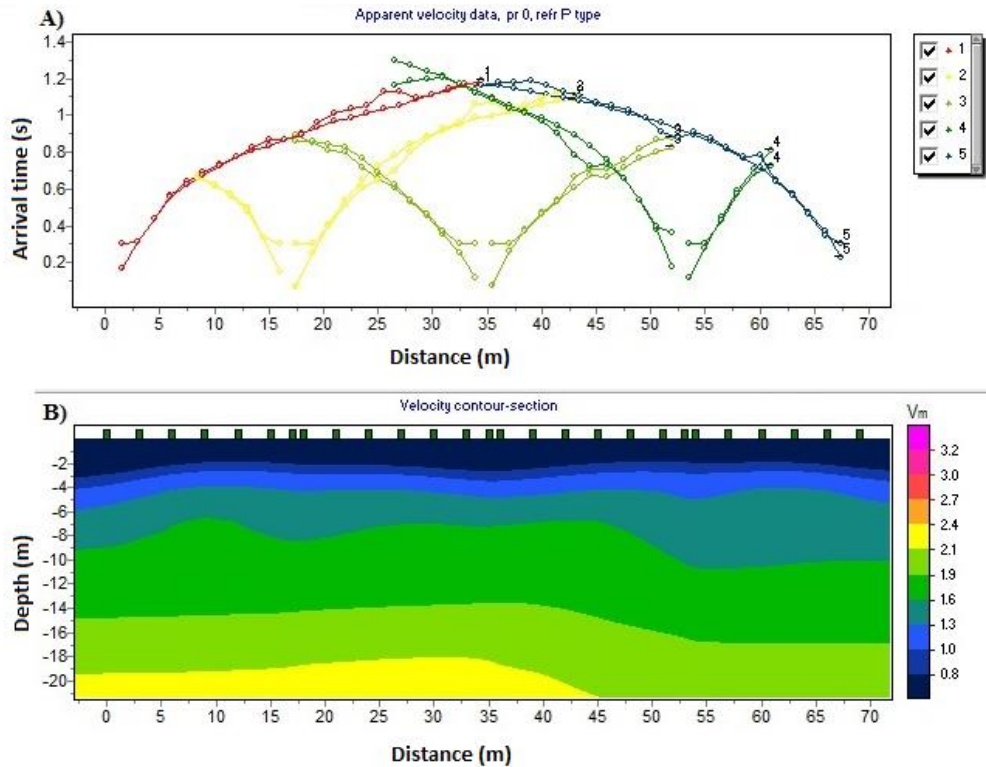


Figure 13. Seismic Refraction Profile P4.

A. Arrival times of the seismic waves as received by the geophones, plotted in time and distance.

B. Velocity model. The yellow horizon represents the “Carbonates” in the Figures 11 and 12. The blue and green horizons represent the overlying clastic rocks.

5. Interpretation

Both the bedded and debris carbonates contain micrite and similar bioclasts. This encourages the interpretation that the coral-bioclasic limestone is the source of the material found in the debris facies which has been reworked downslope. The high micrite content further suggests that the debris was transported down-slope as a cohesive flow, at a stage during which the micrite was still lime mud, providing for a muddy transport medium with some shear strength (debris flow deposit). This interpretation is consistent with the associated erosional truncation surface at the base (eastern outcrop) and an onlap surface at the top (western outcrop), respectively, as debris flows can scour subjacent sediments, and as debrites may display an irregular surface after cohesive freezing. The debrite indicates that sediment accumulation was unstable at a slope. Other phenomena of slope instability in the Barzaman Formation have been documented at the margins of the car park [7, 25]. They also documented a syndepositional thrust (also at the margin of the car park) within the Barzaman Formation. Syndepositional tectonics and related seismicity may have caused slope instability and triggered the debris flow. Seismicity and increased slope gradients may have formed in the context of ongoing uplift of the Oman Mountains and activity at a major extensional shear zone at the foot of the mountains [19, 20]. The bedded facies represents lagoonal conditions with a typical lagoonal bioclast association. Common micrite is indicative of calm water. Allochems in a lagoon may indicate what the lagoon barrier is mainly composed of. Because of the absence of ooids we rule out that the barrier (or shoal or bank) was composed of ooids. During the Eocene, the subjacent Seeb Formation limestones contains low-relief banks that are largely made up of Nummulites and Assilina tests [26, 27]. We have not seen corresponding foraminifer accumulations in the Barzaman limestones to allow for the assumption that foraminifer shoals or banks may have separated the lagoon from the open sea. Instead the lagoon limestones contain abundant coral colonies which may indicate that the lagoon was separated from the open sea by coral reefs. The limestone beds of both outcrops can be laterally correlated (Figure 14). The lowest limestone bed of the Barzaman Formation is the basal bedded, coralline boundstone layer of the eastern outcrop. Its lateral equivalent in the western outcrop is not exposed (Figure 14). The debrite unit bed is present in both outcrops, displaying a thickness of 7.5 m which is a minimum value as its base is not exposed in either outcrop (Figures 3A and 6). In both outcrops, this debrite layer shares the same sedimentological and compositional characteristics (Tables 1 and 2). These aspects and its stratigraphic position (Figure 14) suggest that this facies represents the same stratigraphic level in both outcrops. Finally, the upper bedded boundstone displays the same thickness of 2.5 m (Figure 14) in both outcrops and features similar bioclasts (Tables 1 and 2).

The correlation between both outcrops is also supported by the seismic refraction survey (Figures 11-13) which revealed a gentle dip of the beds to the east, allowing for the interpretation that the carbonates that are exposed in the west and above the parking lot occur in the east below the parking lot.

GEOLOGY OF THE BARZAMAN FORMATION

5. Béchennec, F., Roger, J., Le Métour, J., and Wyns, R. Geological Map of Seeb, Sheet NF40-03, Scale 1:250.000, with Explanatory Notes, 1992, 104pp., Oman Ministry of Petroleum and Minerals, Directorate General of Minerals.
6. Winterleitner, G., Schütz, F., Wenzlaff, C. and Huenges, E. The Impact of Reservoir Heterogeneities on High-Temperature Aquifer Thermal Energy Storage Systems. A Case Study from Northern Oman. *Geothermics*, 2018, **74**, 150-162.
7. Al-Amri, S., Lithostratigraphy and Facies of Siliciclastics and Carbonates and Their Correlation: the Barzaman Formation (Miocene) at SQU Campus (Al-Khoud, Oman), MSc Thesis, Sultan Qaboos University, 2018, 95 pp.
8. Nolan, S.C., Skelton, P.W., Clissold, B.P. and Smewing, J.D. Maastrichtian to Early Tertiary stratigraphy and paleogeography of the Central and Northern Oman Mountains. In: *The Geology and Tectonics of the Oman Region*, (Eds. Robertson, A.H.F., Ries, M.P. and Ries, A.C.), Geological Society, London, Special Publications, 1990, **49**, 495-519.
9. Scharf, A., Mattern, F. and Al Sadi, S. Kinematics of Post-obduction Deformation of the Tertiary Ridge at Al-Khod Village (Muscat Area, Oman). *Sultan Qaboos University Journal for Science*, 2016, **21(1)**, 26-40.
10. Glennie, K.W., Boeuf, M.G.A., Hughes-Clarke, M.W., Moody-Stuart, M., Pilaar, W.F.H. and Reinhardt, B.M., Late Cretaceous nappes in Oman Mountains and their geological evolution. *American Association of Petroleum Geologists Bulletin*, 1973, **57**, 5-27.
11. Glennie, K.W., Boeuf, M.G.A., Hughes-Clarke, M.W., Moody-Stuart, M., Pilaar, W. and Reinhardt, B.M., Geology of the Oman Mountains. *Verhandelingen van het Koninklijk Nederlands geologisch mijnbouwkundig Genootschap*, 1974, **31**, 1-423.
12. Searle, M.P. and Malpas, J. Structure and metamorphism of rocks beneath the Semail ophiolite of Oman and their significance in ophiolite obduction. *Transactions of the Royal Society of Edinburgh*, 1980, **71**, 247-262.
13. Lippard, S.J., Shelton, A.W. and Gass, I.G. The ophiolite of northern Oman. *Journal of the Geological Society (London) Memoir*, 1986, **11**, 1-178.
14. Searle, M. and Cox, J., 1991. Tectonic setting, origin, and obduction of the Oman ophiolite. *Geological Society of America Bulletin*, 1991, **111**, 104-122.
15. Hacker, B.R., Mosenfelder, J.L. and Gnos, E., 1996. Rapid emplacement of the Oman ophiolite: Thermal and geochronologic constraints. *Tectonics*, 1996, **15**, 1230-1247.
16. Goffé, B., Michard, A., Kienast, J.R. and LeMer, O. A case of obduction related high P, low T metamorphism in upper crustal nappes, Arabian continental margin, Oman: P-T paths and kinematic interpretation. *Tectonophysics*, 1988, **151**, 363-386.
17. Glennie, K.W. *The Geology of the Oman Mountains: An Outline of Their Origin*, 2nd ed., Scientific Press, Beaconsfield, 2005, 1-110.
18. Rollinson, H.R., Searle, M.P., Abbasi, I. A., Al-Lazki, A.I. and Al Kindi, M.H., Introduction. In: Rollinson, H.R., Searle, M.P., Abbasi, I.A., Al-Lazki, A.I., Al Kindi, M.H. (Eds.), *Tectonic Evolution of the Oman Mountains*. Geological Society of London Special Publication, 2014, **392**, 27-37.
19. Hansman, R.J., Ring, U., Thomson, S.N., den Brock, B. and Stübner, K. Late Eocene uplift of the Al Hajar Mountains, Oman, supported by stratigraphic and low-temperature thermochronology. *Tectonics*, 2017, **36**, 3081-3109.
20. Mattern, F. and Scharf, A. Postobductional extension along and within the Frontal Range of the Eastern Oman Mountains. *Journal of Asian Earth Sciences*, 2018, **154**, 369-385.
21. Searle, M.P. Structural geometry, style and timing of deformation in the Hawasina Window, Al Jabal al Akhdar and Saih Hatat culminations, Oman Mountains. *GeoArabia*, 2007, **12**, 99-130.
22. Poupeau, G., Saddiqi, O., Goffé, A.M.B. and Oberhänsli, R. Late thermal evolution of the Oman Mountains subophiolitic windows: apatite fission-track thermochronology. *Geology*, 1998, **26**, 1139-1142.
23. Flügel, E., *Microfacies of Carbonate Rocks*, 2nd ed., Springer, Berlin, 2010, 984pp.
24. Sartorio, D.S., Venturini, S., *Southern Tethys Biofacies*, Agip, 1988, 1-235.
25. Mattern, F., Scharf, A. and Al-Amri, S.H.K. East-west directed Cenozoic compression in the Muscat area (NE Oman): timing and causes. *Gulf Seismic Forum*, 19-22 March 2018, Muscat, Oman, Book of Abstracts, p. 116.
26. Racey, A. A review of Eocene nummulitide accumulations: structure, formation and reservoir potential. *Journal of Petroleum Geology*, 2001, **24**, 79-100.
27. Beavington-Penney, S.J., Wright, V.P. and Racey, A. The Middle Eocene Seeb Formation of Oman: an investigation of acyclicity, stratigraphic completeness, and accumulation rates in shallow marine carbonate settings. *Journal of Sedimentary Research*, 2006, **76**, 1137-1161.

Received 15 September 2019

Accepted 15 March 2020